



Published in final edited form as:

Nature. 2013 September 5; 501(7465): 107–111. doi:10.1038/nature12416.

Induction of intestinal stem cells by R-spondin 1 and Slit2 augments chemoradioprotection

Wei-Jie Zhou¹, Zhen H. Geng¹, Jason R. Spence², and Jian-Guo Geng¹

¹Department of Biologic and Materials Sciences, University of Michigan School of Dentistry, Ann Arbor, MI 48109, USA

²Departments of Cell and Developmental Biology and Internal Medicine, Division of Gastroenterology, University of Michigan School of Medicine, Ann Arbor, MI 48109, USA

Abstract

Cancer research has been righteously and successfully focused on prevention, early detection and identification of specific molecular targets that distinguish the malignant cells from the neighboring benign cells¹. However, a major clinical challenge concerns how we can reduce lethal tissue injury caused by intensive chemoradiotherapy during treatment of late-staged metastatic cancers. Here we tested whether induction of adult stem cells repairs chemoradiation-induced tissue injury and prolongs overall survival. We found that intestinal stem cells (ISCs)² expressed Slit2 and its single-span transmembrane cell-surface receptor Roundabout 1 (Robo1)^{3,4}. Partial genetic deletion of *Robo1* decreased intestinal stem cells (ISCs) and caused villus hypotrophy, whereas *Slit2* transgene increased ISCs and triggered villus hypertrophy. During lethal dosages of chemoradiation, administering a short pulse of R-spondin 1 (Rspo1; a Wnt agonist)^{5–14} plus Slit2 reduced ISC loss, mitigated gut impairment and protected animals from death, without concomitantly decreasing tumor sensitivity to chemotherapy. Rspo1 and Slit2 may thus act as therapeutic adjuvants to enhance host tolerance to aggressive chemoradiotherapy for eradicating metastatic cancers.

We found, by two-color fluorescent *in situ* hybridization (FISH), that Slit2 and Robo1 mRNAs not only co-localized, but also were expressed in markedly higher amounts in the crypts when compared to the villi in the small intestines of adult C57BL/6 (Wt) mice (Fig. 1a and Supplementary Fig. 1a). Ki67⁺-transient amplifying (TA) cells and LGR5⁺-ISCs expressed Slit2 and Robo1 mRNAs (Fig. 1b, c). In contrast, neither Slit2 nor Robo1 mRNA was visible in lysozyme⁺-Paneth cells. Using the intestinal specimens harvested from LGR5-EGFP-IRES-creERT2 (LGR5-GFP) mice¹⁵, we confirmed that Slit2 and Robo1

Users may view, print, copy, download and text and data- mine the content in such documents, for the purposes of academic research, subject always to the full Conditions of use: http://www.nature.com/authors/editorial_policies/license.html#terms

Full address for correspondence: Dr. Jian-Guo Geng, Department of Biologic and Materials Sciences, University of Michigan School of Dentistry, A317 Medical Science Research Building III, 1150 W. Medical Center Drive, Ann Arbor, MI 48109-5632, USA. Tel.: (734) 763-7073. Fax: (734) 763-4450. jgeng@umich.edu.

Supplemental Information is available in the online version of the paper.

Author Contributions W.-J.Z. and Z.H.G. carried out all experiments, collected and analyzed data, J.R.S. contributed *in vitro* intestinal crypt culture, and J.-G.G. proposed hypothesis, designed experiments and wrote the manuscript.

The authors declare competing financial interests.

mRNAs were expressed by GFP^{high}-ISCs at the bottom of the crypt (Fig. 1d). The distribution of Slit2 and Robo1 is apparently higher at the crypts than in the villi of the small intestine, which mirrors the well-characterized gradient of active β -catenin in the crypt-villus axis¹⁶.

Complete or partial genetic deletion of *Robo1* is embryonic lethal while mice with partial genetic deletion of both *Robo1* and 2 are viable^{17,18}. Thus, we examined the intestinal morphology in *Robo1/2* double heterozygotes (*Robo1*^{+/-}; *Robo2*^{+/-} or *Robo1/2* mutants). *Robo1/2* mutants displayed reduced expression of Robo1 protein, but not Slit2 or α -tubulin (tub; Supplementary Fig. 2a). Notably, Robo2 mRNA was not detectable in the Wt small intestine, even though it clearly was present in the cerebellum (Supplementary Fig. 1b). Compared to Wt littermates, *Robo1/2* mutants had noticeably sparser, shorter and floppier villi throughout the entire small intestine (Fig. 2a; Supplementary Fig. 3a), displaying markedly fewer Ki67⁺-TA cells (Fig. 2b), LGR5⁺-ISCs (Fig. 2c), villin⁺-enterocytes (Fig. 2d), and a reduced number of proliferating intestinal cells visualized by bromodeoxyuridine (BrdU) staining (Supplementary Fig. 4a). The mutant animals also had a higher level of endotoxin (Supplementary Fig. 5), a functional indicator of intestinal impairment¹³. Importantly, *Robo1* single heterozygotes (*Robo1*^{+/-} or *Robo1* mutant) phenocopied the *Robo1/2* double heterozygotes (Supplementary Fig. 6a–d), whereas no such alterations were detected in the intestines of *Robo2* single heterozygotes (*Robo2*^{+/-} or *Robo2* mutant; Supplementary Fig. 7a–d). We also isolated intestinal crypts from *Robo1/2* mutants and found that *Robo1*^{+/-}/*2*^{+/-} crypts failed to form intestinal organoids, also called mini-guts or enteroids^{5–8}, as compared to their Wt littermates (Fig. 2e and Supplementary Fig. 8a for enlarged images). The expression of LGR5, CD133, Sox9, Bmi1 and mTert mRNAs as ISC markers¹⁹ was significantly reduced in the *Robo1/2* mutant intestines relative to their Wt counterparts (Supplementary Fig. 9a). As Slit-Robo signaling re-models neovasculature³ and induces epithelial-mesenchymal transition⁴, we examined and found no aberrant localization and distribution of CD31⁺-vascular endothelial cells in the vasculatures, including those distributing alongside the TA compartment and the capillary bed in the villi (Supplementary Fig. 10a, d), or of α -smooth muscle actin⁺-intestinal smooth muscle cells (Supplementary Fig. 11a) in the intestines of *Robo1/2* mutants as compared to their Wt littermates. These data collectively indicate that the Slit2-Robo1 interaction induces ISCs during physiologic maintenance of intestinal homeostasis.

To complement our genetic findings, we used R5, a monoclonal antibody (mAb) that binds to Robo1, but not Robo2–4, and neutralizes Slit2 binding to Robo1^{3,4}. Wt mice were treated daily for 6 days with an intraperitoneal injection of isotype-matched irrelevant mouse IgG (mIgG) or R5. As expected, R5, but not mIgG, reduced intestinal villus size (Supplementary Fig. 12a) and number (Supplementary Fig. 3b), decreased the numbers of Ki67⁺-TA cells (Supplementary Fig. 12b), LGR5⁺-ISCs (Supplementary Fig. 12c), villin⁺-enterocytes (Supplementary Fig. 12d) and BrdU⁺-intestinal cells (Supplementary Fig. 4b), without concomitantly affecting the distributions of vascular endothelial cells (Supplementary Fig. 10b, e) and smooth muscle cells (Supplementary Fig. 11b). Compared to mIgG, R5 potently inhibited the *in vitro* formation of intestinal organoids^{5–8} isolated from Wt mice

(Supplementary Figs. 12e, 8b for enlarged images), the expression of LGR5, CD133, Sox9, Bmi1 and mTert mRNAs¹⁹ (Supplementary Fig. 9b).

We next asked whether ectopically expressed *Slit2* (Robo1 ligand) might augment ISCs and their daughter cells, leading to villus hypertrophy. To this end, we examined the intestinal phenotypic changes in *Slit2* transgenic (*Slit2*-Tg) mice driven by the pCMV promoter for efficient, but non-selective expression of human *Slit2* transgene²⁰. As compared to Wt mice, *Slit2*-Tg mice displayed an increased mosaic expression of Slit2 protein, but not Robo1 or α -tubulin (tub), in the small intestines (Supplementary Fig. 2b). When compared to Wt mice, *Slit2*-Tg mice had noticeably thicker, longer, enlarged and outnumbered villi (Fig. 3a, Supplementary Fig. 3c), with increased numbers of Ki67⁺-TA cells (Fig. 3b), LGR5⁺-ISCs (Fig. 3c), BrdU⁺-intestinal cells (Supplementary Fig. 4c) and villin⁺-enterocytes (Fig. 3d), without concomitantly affecting the distribution of CD31⁺-vascular endothelial cells (Supplementary Fig. 10c, f) or α -smooth muscle actin⁺-smooth muscle cells (Supplementary Fig. 11c). The compartment of Ki67⁺-TA cells appeared to be enlarged, which could be caused by accelerated proliferation (Supplementary Fig. 4c) and/or aberrant directional migration of TA cells triggered by Slit-Robo signaling^{3,4}. Notably, the intestinal crypts isolated from *Slit2*-Tg mice formed more and larger intestinal organoids⁵⁻⁸ relative to their Wt counterparts (Fig. 3e; Supplementary Fig. 8c for enlarged images). Compared to Wt mice, the expression of LGR5, CD133, Sox9, Bmi1 and mTert mRNAs¹⁹ (Supplementary Fig. 9c) was significantly augmented in the small intestine of *Slit2*-Tg mice. Taken together, our results indicate the functional significance of Slit-Robo signaling in intestinal regeneration through modulation of ISCs.

We further tested whether recombinant Slit2 (rSlit2⁴) could substitute and potentiate recombinant Rspo1 (rRspo1; Supplementary Fig. 13a) for inducing intestinal organoids *in vitro*. As predicted, rSlit2 acted synergistically with rRspo1 to promote *in vitro* formation and growth of intestinal organoids in terms of their number and size (Supplementary Figs. 14a, 8d for enlarged images). In the absence of rRspo1 (rRspo1-), rSlit2 alone, at 0.5 or 1 μ g/ml, was capable of inducing intestinal organoids. The intestinal crypts isolated from *Slit2*-Tg mice also formed intestinal organoids without added rRspo1 or rSlit2. Using single cell sorting gated for GFP⁵, we isolated GFP^{high}-ISCs from LGR5-GFP mice¹⁵ and found that rSlit2 by itself induced intestinal organoids (Supplementary Figs. 14b, 8e for enlarged images). More importantly, rSlit2 acted cooperatively with rRspo1 in the formation of intestinal organoids *in vitro*. To further demonstrate whether Slit2 could induce the self-renewal and pluripotential capacities of ISCs, we performed serial passages (up to 4 passages; every two weeks for each passage) of cultured intestinal organoids and found that rSlit2 not only substituted for rRspo1, but also functioned synergistically with rRspo1, using both the isolated Wt intestinal crypts (Supplementary Fig. 15a) and the sorted GFP^{high}-ISCs (Supplementary Fig. 15b).

Considering that LGR5 is a specific ISC marker¹⁵ and a direct targeting gene of canonical Wnt signaling^{2,5-8}, we treated LGR5-GFP mice with mIgG and R5 and found that compared to untreated (normal) or mIgG-treated LGR5-GFP mice, R5 inhibited the number of GFP^{high}-ISCs (~50% inhibition; Supplementary Fig. 16a). Compared to untreated LGR5-GFP mice, treatment with rRspo1 plus rSlit2 increased the number of GFP^{high}-ISCs (~30%

increase; Supplementary Fig. 16b). Treatment with rRspo1 or rSlit2 alone also slightly augmented the number of GFP^{high}-ISCs. Our results thus provide *in vivo* evidence for the biological importance of our newly discovered Slit2 and Rspo1 cooperation in induction of ISCs and activation of Wnt/ β -catenin signaling.

We also tested the functional significance of Robo1 in Rspo1-induced intestinal repair *in vivo*. Consistent with previous reports⁹⁻¹⁴, intravenous administration of rRspo1 potently promoted villus growth in the Wt jejunum (Supplementary Fig. 17a). Surprisingly, rRspo1 (0.1 mg/mouse/day for 5 days) failed to accelerate growth of intestinal epithelial cells in *Robo1/2* mutants. Compared to their rRspo1-treated Wt counterparts, rRspo1 also failed to significantly augment the numbers of LGR5⁺-ISCs (Supplementary Fig. 17b) and Ki67⁺-TA cells (Supplementary Fig. 17c) in the jejunum crypts of *Robo1*^{+/-}; *Robo2*^{+/-} mice. A prolonged pulse of rRspo1 (0.1 mg/mouse/day for 10 days) further robustly enhanced crypt size (Supplementary Fig. 18a) and augmented the numbers of Ki-67⁺-TA cells (Supplementary Fig. 18b), BrdU⁺-intestinal cells (Supplementary Fig. 18c) and LGR5⁺-ISCs (Supplementary Fig. 18d) in Wt littermates, but not in *Robo1/2* mutants. As predicted, treatment of Wt littermates with rRspo1 markedly induced the cytoplasmic and nuclear translocation of β -catenin (Supplementary Fig. 19a) and elevated the expression of c-Myc (Supplementary Fig. 19b) as compared to *Robo1/2* mutants.

Stimulation of Wnt/ β -catenin signaling with Rspo1 can ameliorate 5-FU and radiation-induced gut damage, including radiation-induced gastrointestinal syndrome (RIGS)⁹⁻¹³. Relatedly, we found that the therapeutic dosage of 5-fluorouracil (5-FU)⁹, a well-characterized chemotherapy medicine, drastically shortened the villus length (Supplementary Fig. 20a) and reduced the numbers of LGR5⁺-ISCs (Supplementary Fig. 20b) and Ki67⁺-TA cells (Supplementary Fig. 20c) in the Wt jejunum, but not in the *Slit2*-Tg jejunum. These findings attest to the functional significance of Slit2 for promoting chemotherapy-induced intestinal repair.

Considering our findings that Slit2 potentiated Rspo1-induced ISCs and synergized with Rspo1 for reducing chemotherapy-induced gut injury, we asked whether Slit2, in combination with Rspo1, could induce ISCs and consequently prolong overall survival in mice receiving lethal challenges of chemoradiation. To our surprise, in mice with the *Slit2* transgene, there was a 70% survival rate in mice receiving a lethal dose of 5-FU²¹, whereas this same dosage caused the death of all Wt mice within two weeks (Fig. 4a). The lethal dose of 5-FU abolished >90% GFP^{high}-ISCs (Supplementary Fig. 21a). However, a 3-day treatment of rSlit2 or rRspo1 alone protected ~40% GFP^{high}-ISCs. Most exciting was the finding that the same regiment of rRspo1 plus rSlit2 preserved ~80% GFP^{high}-ISCs. Our findings thus indicate that Slit2 acts synergistically with Rspo1 for cooperative induction of ISCs, leading to prolongation of overall survival in response to the lethal dose of chemotherapy.

Because aberrant Wnt signaling causally contribute to colorectal carcinogenesis², because Slit2 and Robo1 expression inversely correlates with the overall survival rate in colorectal cancer⁴, and because recurrent gene fusion of Rspo2 and 3 contributes to colorectal cancer²², we explored whether a short 3-day pulse of rSlit2 and/or rRspo1 could accelerate

the development of intestinal carcinogenesis and/or decrease its sensitivity to chemoradiotherapy. To test this, *Apc*^{MIN/+} mice with spontaneous intestinal adenoma were treated with dextran sulfate sodium (DSS) to induce inflammation related intestinal carcinogenesis, a murine model that is thought to closely mimic multi-factorial human colorectal cancer²³. Treatment of DSS-treated *Apc*^{MIN/+} mice with rSlit2 or rRspo1 alone led to a 20–30% survival rate upon the lethal dosage of 5-FU (Fig. 4b). Importantly, a combination of rSlit2 and rRspo1 led to a 60% survival rate ($p=0.0023$ between the rRspo1 plus rSlit2 group compared to either group alone), demonstrating the functional cooperation between Slit2 and Rspo1 leading to increased host tolerance to the lethal dose of chemotherapy in this murine model of carcinogenesis.

Consistent with previous reports using recombinant flagellin in xenografted mouse sarcoma and malignant melanoma²⁴ and adenoviral Rspo1 in xenografted human colorectal carcinoma¹², neither acceleration of intestinal cancer development nor desensitization to 5-FU chemotherapy was detected with our rRspo1 and rSlit2 combination treatment (Fig. 4c). In contrast, upon administration of rRspo1 and rSlit2, a single “lethal” dose of 5-FU drastically eliminated the number of intestinal tumors, suggesting that Rspo1 plus Slit2 treatment may act as adjuvants before, during or after intensive chemotherapy for cancer eradication.

Furthermore, the combination of rSlit2 plus rRspo1 led to a 30% survival rate in mice receiving a lethal dose of whole body irradiation (WBI; Fig. 4d) and a 50% survival rate in mice receiving a lethal dose of abdominal irradiation (AIR; Fig. 4h). We also observed concomitant prolongations of the villus length (Fig. 4e, i), augmentations of LGR5⁺-ISCs (Fig. 4f, j) and Ki67⁺-TA cells (Fig. 4g, k) in the jejunum, which are in analogous to previous finding that LGR5⁺-ISCs in the small intestine are resistant to radiation²⁵. Mechanistically, although the lethal dose of WBI abolished >80% GFP^{high}-ISCs (Supplementary Fig. 21b), a 3-day treatment of rRspo1 or rSlit2 alone protected ~40% GFP^{high}-ISCs while rRspo1 plus rSlit2 preserved >80% GFP^{high}-ISCs in LGR5-GFP mice.

In summary, our study indicates that Slit2 and Rspo1 cooperatively induce ISC for intestinal homeostasis and repair and significantly prolong overall survival following lethal doses of chemoradiotherapy. To the best of our knowledge, the combined Slit2/Rspo1 treatment, used as an adjuvant approach, is the first example to demonstrate the feasibility of inducing endogenous adult tissue-specific stem cells for organ and tissue repair with far-reaching medical impact.

METHODS

Mouse experiments and histology

C57BL6/J (Wt; Stock No. 005304), LGR5-EGFP-IRES-creERT2 (LGR5-GFP; Stock No. 008875)¹⁵, and *Apc*^{MIN/+} (Stock No. 002020) mice were purchased from Jackson Laboratory. *Robo1*^{+/-}; *Robo2*^{+/-} mice^{17,18} were purchased from MMRRC/University of Missouri and their Wt littermates were used as controls. During the process of expanding our cohort of *Robo1*^{+/-}; *Robo2*^{+/-} mice, we unexpectedly obtained several adult single *Robo1* (*Robo1*^{+/-}; less than 3% of total mouse population) or *Robo2* (*Robo2*^{+/-})

heterozygotes that were not embryonically lethal. Notably, we have never obtained any viable *Robo1*^{-/-} homozygotes after multiple trials. *Slit2*-Tg mice were generated and characterized as described²⁰. Male and female mice were equally divided without randomization. They were used at 8 weeks old unless specifically indicated. For measurement of cell proliferation, mice were injected with BrdU (1 mg/100 grams of body weight) for 2 h prior to sacrifice. For antibody treatment, Wt mice were injected intraperitoneally with isotype-matched irrelevant mIgG or R5 monoclonal Ab^{3,4} (1 mg/mouse/day for 6 consecutive days). For induction of inflammation-related intestinal carcinogenesis, *Apc*^{MIN/+} mice were treated with 2% dextran sulfate sodium (DSS) in drinking water for one week and were used experimentally two weeks later²³. For “chemoradiation” experiments, Wt and DSS-treated *Apc*^{MIN/+} mice (10 weeks old) were injected intravenously with *Slit2* or *Rspo1* alone or in combination (0.1 mg/mouse/day for 3 consecutive days). On day 2, they were given 5-FU intraperitoneally (30 mg/kg/mouse/day for 5 days for the therapeutic dose⁹ or 300 mg/kg once for the lethal high dose²¹) or were irradiated (10.4 Gy/mouse once for WBI or 12 Gy/mouse once for AIR¹²). Alternatively, *Slit2*-Tg mice²⁰ (10 weeks old) were given the lethal high dose of 5-FU intraperitoneally (300 mg/kg once²¹). Tissue sections of small intestines were stained with hematoxylin & eosin (H&E) and the relative villus sizes and numbers at the duodenum, jejunum and ileum were double-blindly measured. The length ratios of 1:3:2 of the entire small intestine were defined as the duodenum, jejunum and ileum²⁶, respectively. Serum LPS levels were measured using the limulus amebocyte lysate assay (Lonza). Mouse experiments were approved by the University Committee on Use and Care of Animals (UCUCA) of the University of Michigan.

Fluorescent in situ hybridization

cDNA segments of mouse *Slit2* (base pair 3960–4566), mouse *Robo1* (base pair 3443–4956) and mouse *Robo2* (base pair 2328–4527) were reverse transcribed and labeled with digoxigenin (DIG) or biotin according to the manufacturer’s instructions (Roche). Intestinal tissues were fixed with 4% paraformaldehyde and tissue sections (5- μ m thick) were incubated with 1 μ g/ml linearized DIG- or biotin-labeled antisense or sense RNA probe²⁷. For immunofluorescent staining, Western Blocking Reagent (11921673001, Roche) was diluted 1 to 10 with 20 mM Tris-HCl, pH 7.4, containing 0.1% Tween-20 (TBST) for blocking non-specific staining and for diluting all antibodies, including 1:1000 dilution of sheep anti-DIG Ab (11333089001, Roche) or mouse anti-biotin mAb (200-002-211, Jackson ImmunoResearch), and 1:200 dilution of HRP-conjugated rabbit anti-sheep Ab (313-035-047, Jackson ImmunoResearch). Tyramide Signal Amplification Kits (Alexa Fluor 488 and 555; Invitrogen) were used according to the manufacturer’s protocol.

Immunofluorescent and immunohistochemical Staining

Intestinal tissues were fixed with 4% paraformaldehyde, sectioned (5- μ m thick) and permeabilized with 0.05% Triton X-100 in phosphate buffered saline, pH 7.4 (PBS). Samples were blocked with 1% bovine serum albumin (BSA; Sigma) and incubated with primary Ab at 37°C for 1 h, including Abs against Ki67 (ab15580, abcam), LGR5 (ab75850, abcam), lysozyme (ab36362, abcam), CD31 (ab28364, abcam), α -smooth muscle actin (ab5694, abcam), villin (610358, BD Biosciences), c-Myc (sc-40, Santa Cruz

Biotechnology), GFP (NB600-303, Novus Biologicals) and BrdU (B2531, Sigma Aldrich). After washing extensively, samples were incubated with appropriate fluorescent dye- or HRP-conjugated secondary Ab at 37°C for 1 hour. Sections were counterstained with 4',6-diamidino-2-phenylindole (DAPI) or H&E. Slides were then washed and mounted for observation under a scanning confocal microscope (Leica TCS SP2) or a fluorescence stereomicroscope (Leica M205 FA). The immunohistochemical staining data were quantified double blindly using ImageTool Software.

***In vitro* culture of intestinal crypts**

The intestinal crypts of mouse small intestines were isolated²⁸ and cultured *in vitro*^{5–8}. Specifically, mouse ileums (~6 cm) were dissected out of the animals, flushed with ice-cold sterile PBS, cut open lengthwise and into 1 cm pieces, and transferred into the Petri dish with ice-cold sterile PBS supplemented with 1% Pen/Strep (Invitrogen). This step was repeated twice. They were then transferred to a 50-ml conical tube containing 30 ml of ice-cold sterile shaking buffer (PBS supplemented with 15 mM EDTA and 1% Pen/Strep) and rocked in the cold room for 30 minutes, then vortexed at maximal speed for a total of 2 minutes in 30 second intervals. The shaking buffers containing separated crypts were filtered through a 70- μ m filter into a new 50-ml conical tube, counted, transferred to a round-bottom tube (500 crypts/tube), and centrifuged at 200g at 4°C for 10 minutes. After gently removing the supernatant, the crypt pellets were resuspended in 20 μ l of the gut media [Advanced DMEM/F12, 1% L-glutamine, 1% Pen/Strep, 10 μ M HEPES (all from Invitrogen), 1% N2 supplement (R&D Systems), 2% B27 supplement (Invitrogen), 0.5 μ g/ml rRspo1 (Supplementary Fig. 13b), 0.1 μ g/ml rNoggin (Supplementary Fig. 14b), 0.1 μ g/ml EGF (R&D Systems), 0.1 μ g/ml rWnt3a (R&D Systems), or 0.5 or 1 μ g/ml rSlit2⁴]. These crypts were mixed with ice-cold 50 μ l Matrigel (BD Biosciences) and plated onto one well of the 24-well cell culture plate, using a pre-chilled pipette tip. The plate was placed in the 37°C incubator for 30 minutes and an aliquot of 0.5 ml gut media was overlaid. The media was replaced every 2–4 days.

Isolation and cell sorting of GFP-positive ISCs expressing LGR5-GFP was performed according to the previous publication¹⁰. Specifically, the small intestinal crypts of LGR5-GFP mice were isolated and dissociated with TrypLE express (Invitrogen) and 2,000 U/ml DNase (Sigma Aldrich) at 37°C for 30 min. Dissociated cells were passed through a 20- μ m cell strainer and washed with sterile PBS. GFP^{high}-ISCs were isolated using Moflo cell sorter. An aliquot of 10,000 sorted GFP^{high}-ISCs were suspended in 20 μ l gut media, mixed well with 50 μ l Matrigel, and transferred to one well of 24-well plate. The plate was placed in the 37°C incubator for 30 minutes and an aliquot of 0.5 ml gut media supplemented with Y-27632 (10 μ M, to prevent anoikis; Sigma Aldrich) was overlaid. The efficiency of organoids generation from isolated GFP^{high}-ISCs was ~3%, which was similar to the previous reports^{5,29}. Indicated growth factors were added every other day and the entire medium was changed every 4 days. For serial passage, the cultured intestinal organoids were removed from the Matrigel culture and mechanically dissociated into the single crypt domains. After mixing with gut media and Matrigel, they were transferred to the new well and an aliquot of 0.5 ml gut media was overlaid. This procedure was repeated during a two week period, without loss of replicating efficiency.

Isolation and quantitation of GFP⁺-ISCs

The small intestinal crypts of LGR5-GFP mice were isolated and dissociated with TrypLE express (Invitrogen) and 2,000 U/ml DNase (Sigma Aldrich) at 37°C for 30 min. Dissociated cells were passed through a 20- μ m cell strainer and washed with sterile PBS. GFP^{high}-ISCs were stained with the anti-GFP Ab (NB600-303, Novus Biologicals), followed by an appropriate FITC-conjugated secondary Ab for quantification by flow cytometry.

qRT-PCR

All mouse RT² qPCR primer pairs were purchased from SA Biosciences. The crypts of mouse small intestine were isolated²⁸ for qRT-PCR as previously described⁴. Notably, we routinely isolated less amounts of total mRNAs from the atrophied *Robo1*^{+/-}/*2*^{+/-} and R5-treated intestines and more amounts of total mRNAs from the hypertrophied *Slit2*-Tg intestines than the Wt intestines (data not shown). However, the adjusted amounts of total isolated mRNAs were used as the starting materials in the identical quantity for the purpose of comparison.

Immunoblotting

The isolated intestinal crypts were washed with ice-cold phosphate buffered saline, pH 7.4 (PBS) and lysed with ice-cold radioimmunoprecipitation assay lysis buffer [50 mM Tris-HCl, pH 7.4, 150 mM NaCl, 1 mM sodium orthovanadate 10 mM sodium fluoride, 1 mM phenylmethylsulfonyl fluoride, 2 μ g/ml aprotinin, 2 μ g/ml leupeptin, 1 μ g/ml pepstatin A, 15 μ g/ml benzamidine, 0.5% Nonidet P-40, 0.15% bovine serum albumin (BSA) and 10% glycerol] at 4°C for 1 h. Samples were centrifuged at 12,000g for 15 min at 4°C. Samples were subjected to SDS-PAGE, transferred to PVDF membranes (EMD Millipore) and detected with appropriate primary Abs followed by horseradish peroxidase-conjugated goat anti-mouse or rabbit immunoglobulin G (IgG). The blotting signals were detected using SuperSignal West Dura Extended Duration Substrate (Pierce). Quantitative analyses of immunoblotting signals on Fuji Films were obtained by densitometry analysis using LAS4000 Image Software. Notably, we routinely isolated less amounts of total proteins from the atrophied *Robo1*^{+/-}; *Robo2*^{+/-} and R5-treated intestines and more amounts of total proteins from the hypertrophied *Slit2*-Tg intestines than the Wt intestines (data not shown). However, the adjusted amounts of total isolated proteins were used as the starting materials in the identical quantity for the purpose of comparison. The primary Abs against pan-Slit and Robo1 (S1 and R4^{3,4}), α -tubulin (T6074, Sigma Aldrich) and β -actin (A1978, BD Biosciences) were used.

Baculovirus expression of Rspo1 and Noggin

The cDNAs of human Rspo1 and Noggin (Open Biosystems) were amplified for construction of 6-His fusion proteins, using the forward primer 5'-TTGCGGCCGCATGCGGCTTGGGCTGTG-3' and the reverse primer 5'-GGGAATTCGGCAGGCCCTGCAGATGTGAGTGCC-3' for Rspo1; and the forward primer 5'-TAGCGGCCGCATGGAGCGCTGCCCC-3' and the reverse primer 5'-GGGAATTCGCACGAGCACTTGCCTCGGAATGATGG-3' for Noggin. The inserts of

Rspo1 and noggin were digested with NotI/EcoRI. They were ligated into the pVL1392 vector (BD Pharmingen).

Recombinant Rspo1 and Noggin were expressed in Sf9 insect cells using the baculovirus expression system (BaculoGold; BD Pharmingen) and purified to homogeneity from the serum-free supernatant of Sf9 cells infected with their respective viral stocks (MOI ~2 ×10⁸/ml) by Talon metal affinity chromatography (BD Clontech)³⁰. Endotoxin levels of these isolated recombinant proteins were <0.1 unit/mg of proteins measured by limulus amoebocyte lysate (LAL) from Cape Cod.

Statistical analysis

The experimental data were statistically analyzed by Student's *t*-test or Mann-Whitney test. Kaplan-Meier survival curves were constructed and analyzed by a log rank test. The *p* value less than 0.05 or 0.01 was considered statistically significant or very significant, respectively.

Supplementary Material

Refer to Web version on PubMed Central for supplementary material.

Acknowledgements

We thank Li Ma for generating recombinant proteins, Michael H. Geng for technical assistances, Xuesong Yang for helping with the *in situ* hybridization, and Judith Connert for critical reading of the manuscript. This work was supported by grants from the National Institutes of Health (CA126897 and CA181039 to J.- G.G.).

References

1. Hanahan D, Weinberg RA. Hallmarks of cancer: the next generation. *Cell*. 2011; 144:646–674. [PubMed: 21376230]
2. Clevers H, Nusse R. Wnt/β-catenin signaling and disease. *Cell*. 2012; 149:1192–1205. [PubMed: 22682243]
3. Wang B, Xiao Y, Ding B, Zhang N, Yuan X, Gui L, Qian K, Duan S, Chen Z, Rao Y, et al. Induction of tumor angiogenesis by Slit-Robo signaling and inhibition of cancer growth by blocking Robo activity. *Cancer Cell*. 2003; 4:19–29. [PubMed: 12892710]
4. Zhou WJ, Geng ZH, Chi S, Zhang W, Niu XF, Lan SJ, Ma L, Yang X, Wang LJ, Ding YQ, et al. Slit-Robo signaling induces malignant transformation through Hakai-mediated E-cadherin degradation during colorectal epithelial cell carcinogenesis. *Cell Res*. 2011; 21:609–626. [PubMed: 21283129]
5. Sato T, Vries RG, Snippert HJ, van de Wetering M, Barker N, Stange DE, van Es JH, Abo A, Kujala P, Peters PJ, et al. Single Lgr5 stem cells build crypt-villus structures in vitro without a mesenchymal niche. *Nature*. 2009; 459:262–265. [PubMed: 19329995]
6. Ootani A, Li X, Sangiorgi E, Ho QT, Ueno H, Toda S, Sugihara H, Fujimoto K, Weissman IL, Capecchi MR, Kuo CJ. Sustained in vitro intestinal epithelial culture within a Wnt-dependent stem cell niche. *Nat. Med*. 2009; 15:701–706. [PubMed: 19398967]
7. Jung P, Sato T, Merlos-Suárez A, Barriga FM, Iglesias M, Rossell D, Auer H, Gallardo M, Blasco MA, Sancho E, et al. Isolation and in vitro expansion of human colonic stem cells. *Nat. Med*. 2011; 17:1225–1227. [PubMed: 21892181]
8. Spence JR, Mayhew CN, Rankin SA, Kuhar MF, Vallance JE, Tolle K, Hoskins EE, Kalinichenko VV, Wells SI, Zorn AM, et al. Directed differentiation of human pluripotent stem cells into intestinal tissue in vitro. *Nature*. 2011; 470:105–109. [PubMed: 21151107]

9. Kim KA, Kakitani M, Zhao J, Oshima T, Tang T, Binnerts M, Liu Y, Boyle B, Park E, Emtage P, et al. Mitogenic influence of human R-spondin1 on the intestinal epithelium. *Science*. 2005; 309:1256–1259. [PubMed: 16109882]
10. Zhao J, De Vera J, Narushima S, Beck EX, Palencia S, Shinkawa P, Kim KA, Liu Y, Levy MD, Berg DJ, et al. R-Spondin1, a novel intestinotrophic mitogen, ameliorates experimental colitis in mice. *Gastroenterology*. 2007; 132:1331–1343. [PubMed: 17408649]
11. Zhao J, Kim KA, De Vera J, Palencia S, Wagle M, Abo A. R-Spondin1 protects mice from chemotherapy or radiation-induced oral mucositis through the canonical Wnt/ β -catenin pathway. *Proc. Natl. Acad. Sci. USA*. 2009; 106:2331–2336. [PubMed: 19179402]
12. Bhanja P, Saha S, Kabarriti R, Liu L, Roy-Chowdhury N, Roy-Chowdhury J, Sellers RS, Alfieri AA, Guha C. Protective role of R-spondin1, an intestinal stem cell growth factor, against radiation-induced gastrointestinal syndrome in mice. *PLoS One*. 4:e8014. [PubMed: 19956666]
13. Takashima S, Kadowaki M, Aoyama K, Koyama M, Oshima T, Tomizuka K, Akashi K, Teshima T. The Wnt agonist R-spondin1 regulates systemic graft-versus-host disease by protecting intestinal stem cells. *J. Exp. Med*. 2011; 208:285–294. [PubMed: 21282378]
14. de Lau W, Barker N, Low TY, Koo BK, Li VS, Teunissen H, Kujala P, Haegerbarth A, Peters PJ, van de Wetering M, et al. Lgr5 homologues associate with Wnt receptors and mediate R-spondin signalling. *Nature*. 2011; 476:293–297. [PubMed: 21727895]
15. Barker N, van Es JH, Kuipers J, Kujala P, van den Born M, Cozijnsen M, Haegerbarth A, Korving J, Begthel H, Peters PJ, et al. Identification of stem cells in small intestine and colon by marker gene Lgr5. *Nature*. 2007; 449:1003–1007. [PubMed: 17934449]
16. Solanas G, Battle E. Control of cell adhesion and compartmentalization in the intestinal epithelium. *Exp. Cell Res*. 2011; 317:2695–2701. [PubMed: 21820431]
17. Grieshammer U, Le Ma, Plump AS, Wang F, Tessier-Lavigne M, Martin GR. SLIT2-mediated ROBO2 signaling restricts kidney induction to a single site. *Dev. Cell*. 2004; 6:709–717. [PubMed: 15130495]
18. Long H, Sabatier C, Ma L, Plump A, Yuan W, Ornitz DM, Tamada A, Murakami F, Goodman CS, Tessier-Lavigne M. Conserved roles for Slit and Robo proteins in midline commissural axon guidance. *Neuron*. 2004; 42:213–223. [PubMed: 15091338]
19. Yan KS, Chia LA, Li X, Ootani A, Su J, Lee JY, Su N, Luo Y, Heilshorn SC, Amieva MR, et al. The intestinal stem cell markers Bmi1 and Lgr5 identify two functionally distinct populations. *Proc. Natl. Acad. Sci. USA*. 2012; 109:466–471. [PubMed: 22190486]
20. Ye BQ, Geng ZH, Ma L, Geng JG. Slit2 regulates attractive eosinophil and repulsive neutrophil chemotaxis through differential srGAP1 expression during lung inflammation. *J. Immunol*. 2010; 185:6294–6305. [PubMed: 20944010]
21. Martine DS, Stolfi RL, Sawyer RC, Sawyer RC, Spiegelman S, Young CW. High-dose 5-fluorouracil with delayed uridine“rescue” in mice. *Cancer Res*. 1982; 42:3964–3970. [PubMed: 7104997]
22. Seshagiri S, Stawiski EW, Durinck S, Modrusan Z, Storm EE, Conboy CB, Chaudhuri S, Guan Y, Janakiraman V, Jaiswal BS, et al. Recurrent R-spondin fusions in colon cancer. *Nature*. 2012; 488:660–664. [PubMed: 22895193]
23. Phutthaphadoong S, Yamada Y, Hirata A, Tomita H, Hara A, Limtrakul P, Iwasaki T, Kobayashi H, Mori H. Chemopreventive effect of fermented brown rice and rice bran (FBRA) on the inflammation-related colorectal carcinogenesis in Apc^{Min/+} mice. *Oncol. Rep*. 2012; 23:53–59. [PubMed: 19956864]
24. Burdelya LG, Krivokrysenko VI, Tallant TC, Strom E, Gleiberman AS, Gupta D, Kurnasov OV, Fort FL, Osterman AL, Didonato JA, et al. An agonist of toll-like receptor 5 has radioprotective activity in mouse and primate models. *Science*. 2008; 320:226–230. [PubMed: 18403709]
25. Hua G, Thin TH, Feldman R, Haimovitz-Friedman A, Clevers H, Fuks Z, Kolesnick R. Crypt base columnar stem cells in small intestines of mice are radioresistant. *Gastroenterology*. 2012; 143:1266–1276. [PubMed: 22841781]
26. Duan LP, Wang HH, Wang DQ. Cholesterol absorption is mainly regulated by the jejunal and ileal ATP-binding cassette sterol efflux transporters Abcg5 and Abcg8 in mice. *J. Lipid Res*. 2004; 45:1312–1323. [PubMed: 15102882]

27. Yang X, Chrisman H, Weijer CJ. PDGF signalling controls the migration of mesoderm cells during chick gastrulation by regulating N-cadherin expression. *Development*. 2008; 135:3521–3530. [PubMed: 18832396]
28. Booth C, O’Shea JA, Potten CS. Maintenance of functional stem cells in isolated and cultured adult intestinal epithelium. *Exp. Cell Res.* 1999; 249:359–366. [PubMed: 10366435]
29. Merlos-Suárez A, Barriga FM, Jung P, Iglesias M, Céspedes MV, Rossell D, Sevillano M, Hernando-Momblona X, da Silva-Diz V, Muñoz P, et al. The intestinal stem cell signature identifies colorectal cancer stem cells and predicts disease relapse. *Cell Stem Cell*. 2011; 8:511–524. [PubMed: 21419747]
30. Wang HB, Wang JT, Zhang L, Geng ZH, Xu WL, Xu T, Huo Y, Zhu X, Plow EF, Chen M, Geng JG. P-selectin primes leukocyte integrin activation during inflammation. *Nat. Immunol.* 2007; 8:882–892. [PubMed: 17632516]

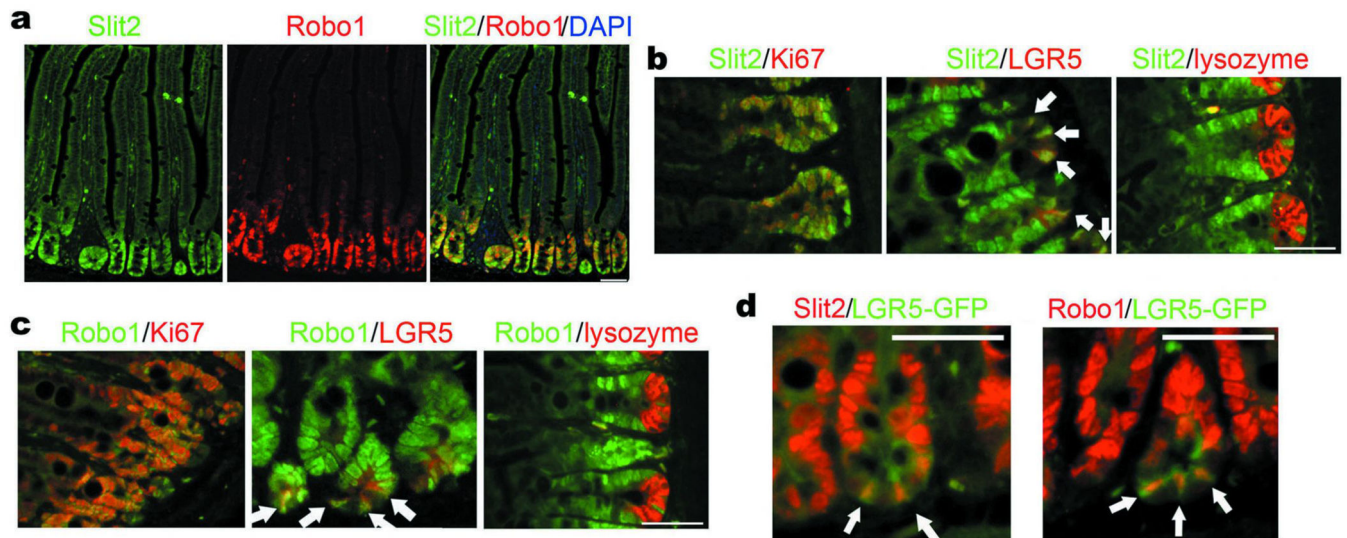


Figure 1. Expression of Slit2 and Robo1 in mouse small intestine

a, Expression and co-localization of Slit2 and Robo1 mRNAs in the crypts of small intestine. Slit2 and Robo1 mRNAs in the Wt small intestines were detected by using the DIG- or biotin-conjugated antisense Slit2 and Robo1 mRNA probes. Slides were counterstained with DAPI. Immunofluorescent images were observed under a laser scanning confocal microscope, and the recorded fluorescent images were then merged. **b–d**, Cellular distribution of mRNAs for Slit2 (**b** and **d**) and Robo1 (**c** and **d**). Slit2, Robo1, Ki67 (a marker for proliferating TA cells), LGR5 (a marker for ISCs), and lysozyme (a marker for Paneth cells) were found at the crypt of small intestines using FISH (Slit2 and Robo1) and immunofluorescent staining with their respective Abs (Ki67, LGR5 and lysozyme). Alternatively, the intestinal tissues isolated from LGR5-GFP mice were stained by the anti-GFP Ab to detect GFP^{high}-cells (**d**). White arrows indicate LGR5⁺-cells (**a–c**) and GFP^{high}-cells (**d**) co-localized with Slit2 or Robo1 mRNA. Results represent at least three separate experiments (five mice/group; 8 weeks old). Bars, 50 μ m for **a–d**.

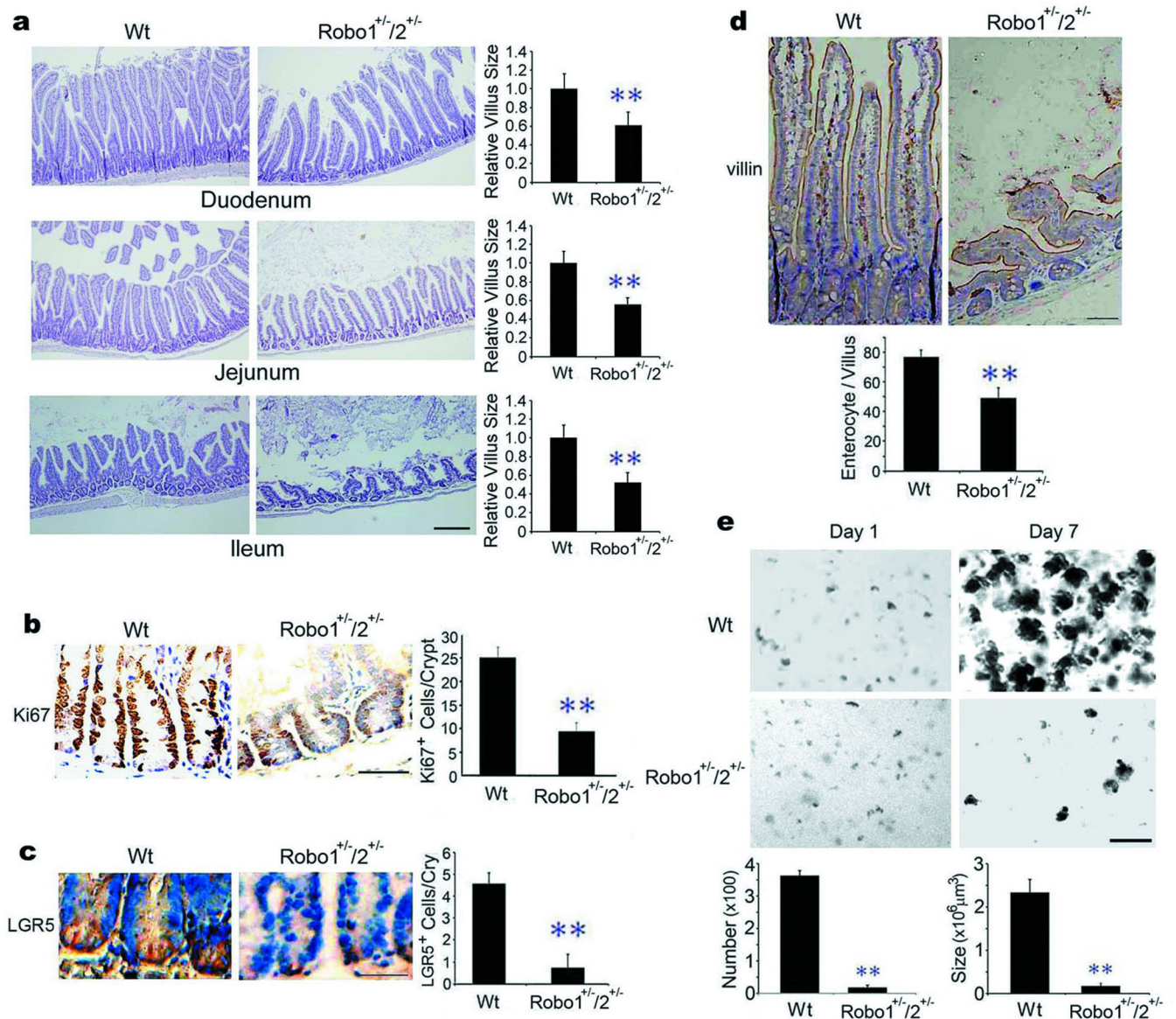


Figure 2. Phenotypic aberration in *Robo1*^{+/-}; *Robo2*^{+/-} small intestine

a, Morphology of small intestines. Paraffin-embedded intestinal sections from Wt littermates (Wt) and *Robo1/2* mutants were stained with hematoxylin & eosin (H&E). Relative villus sizes were measured and statistically analyzed. **b–d**, Effects of partial *Robo1/2* deficiency on intestinal cells. Intestinal sections from Wt littermates and *Robo1/2* mutants were immunohistochemically stained for Ki67⁺-TA cells (**b**), LGR5⁺-ISCs (**c**) and villin⁺-enterocytes (**d**). The numbers of positive cells were counted in each crypt (**b–d**). **e**, Formation of intestinal organoids. The intestinal crypts isolated from Wt littermates and *Robo1/2* mutants were cultured and the numbers and sizes of intestinal organoids were measured at day 7. Results represent fifty tissue specimens in each group (n=5) and the mean ± S.D. values. Bars, 200 μm for **a**, **e** and 50 μm for **b–d**. **, *p*<0.01.

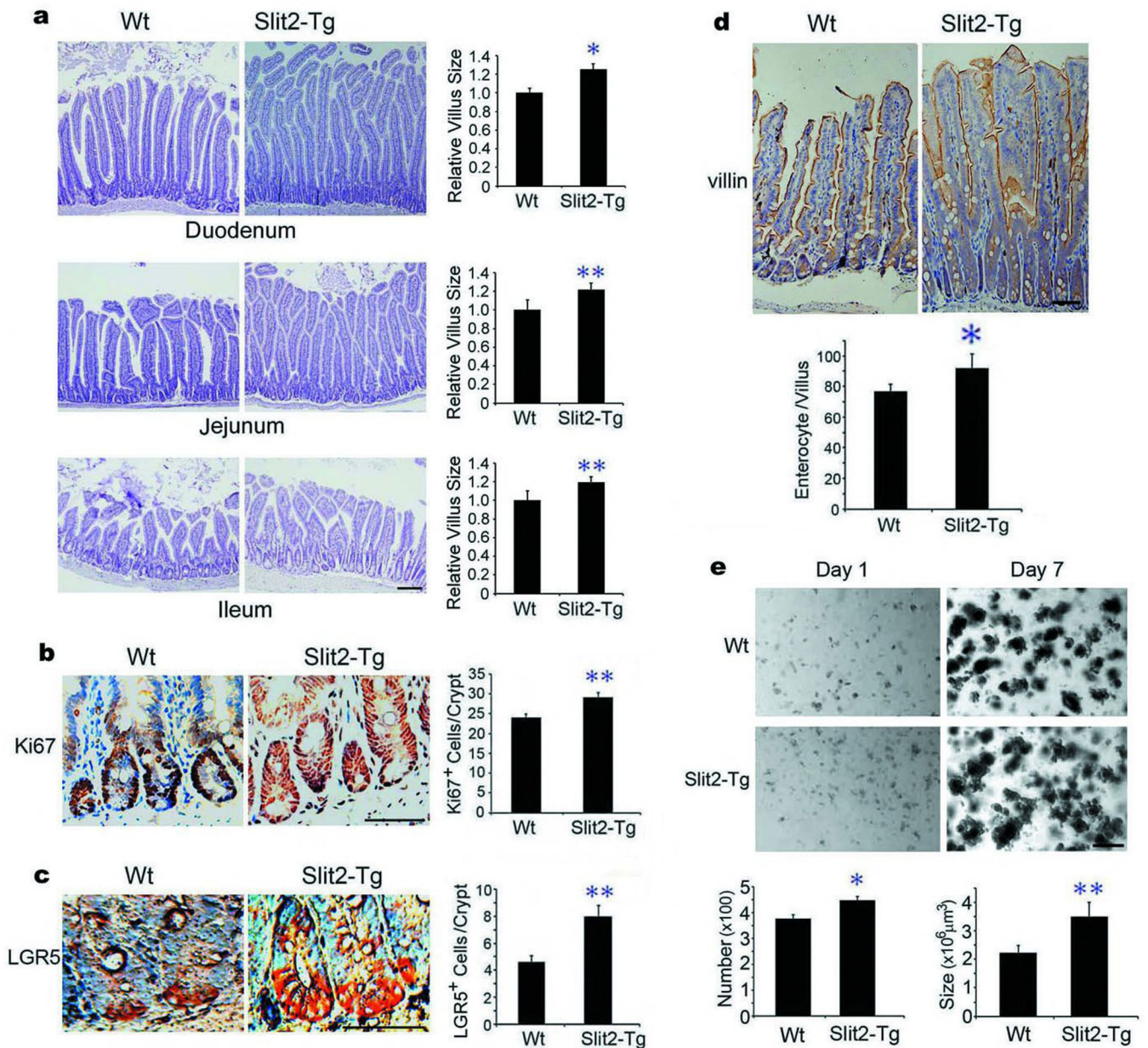


Figure 3. *Slit2* transgene enhances small intestinal regeneration

a, Effects of *Slit2* overexpression on intestinal morphology. Small intestines from Wt and *Slit2*-Tg mice were stained with H&E, and the relative villus sizes were measured and statistically analyzed. **b–d**, Ectopic *Slit2* expression affects the number and distribution of intestinal cells. Small intestines from Wt and *Slit2*-Tg mice were immunohistochemically stained for Ki67⁺-TA cells (**b**), LGR5⁺-ISCs (**c**) and villin⁺-enterocytes (**d**). The numbers of positive cells were counted in each crypt. **e**, The intestinal crypts isolated from Wt and *Slit2*-Tg mice were *in vitro* cultured and the numbers and sizes of intestinal organoids were measured at day 7. Results represent fifty tissue specimens in each group (five mice/group) and the mean ± S.D. of 10 tissue sections/mouse. Bars, 100 μm for **a**, **e** and 50 μm for **b–d**. *, $p < 0.05$; **, $p < 0.01$.

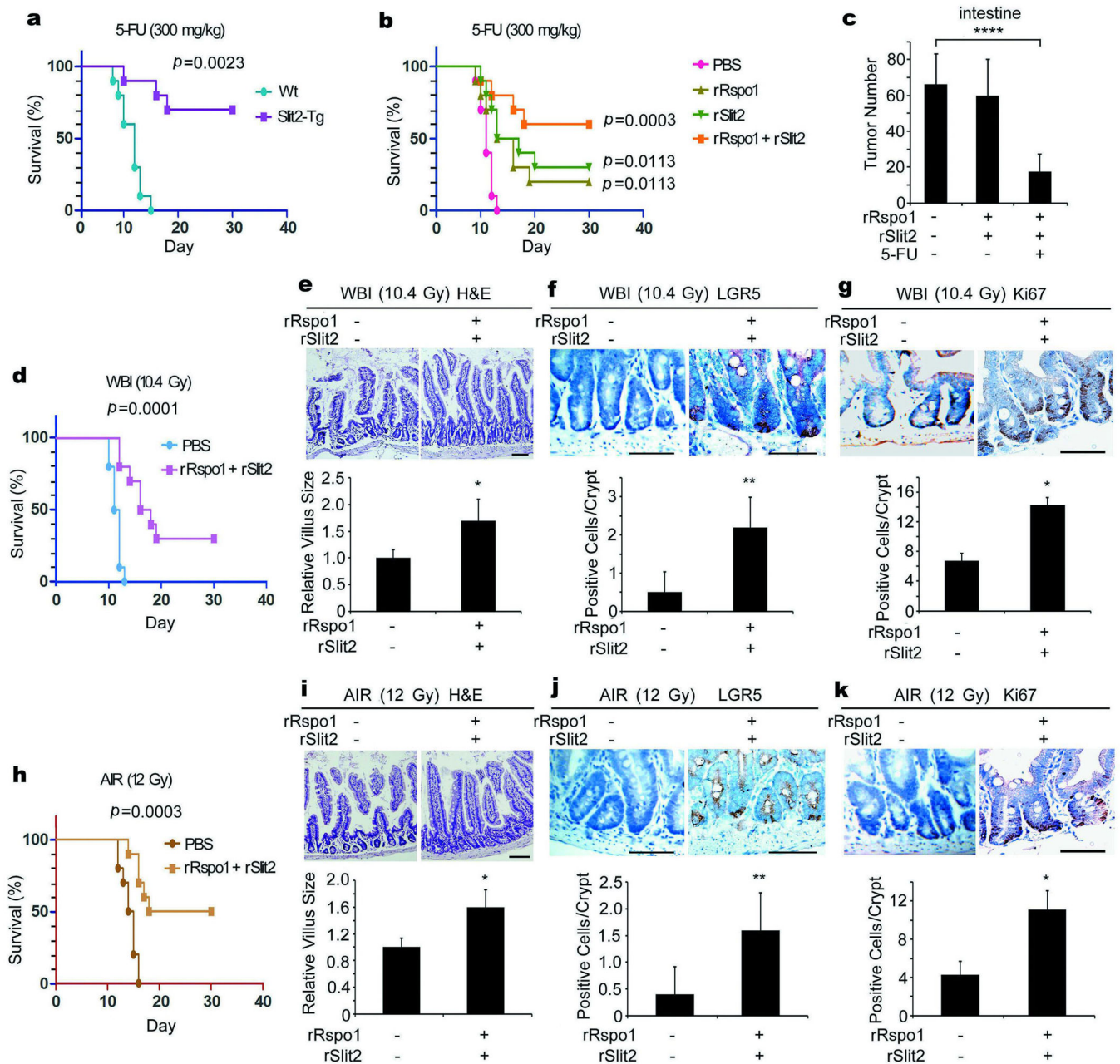


Figure 4. Slit2 and Rspo1 cooperatively induce ISCs, reduce intestinal damage and prolong overall survival

a. *Slit2* transgene increases resistance to 5-FU. A single lethal dose of 5-FU was given to Wt and *Slit2*-Tg mice and the death rates were recorded. **b, c.** Slit2 plus Rspo1 prolongs overall survival in tumor-bearing mice. rSlit2 or rRspo1 alone or in combination were given intravenously to DSS-treated *Apc*^{MIN/+} mice for 3 days. On day 2, a single lethal dose of 5-FU was given and the death rates were recorded (**b**). The tumor numbers in the small intestines of surviving mice were also counted at day 30 (**c**). **d–k.** Slit2 plus Rspo1 decreases radiation-induced death. Wt mice were treated with rSlit2 plus rRspo1. On day 2, they were irradiated and the death rates were recorded (**d, h**). The villus sizes (**e, i**), the numbers of

LGR5⁺-ISCs (**f, j**), and Ki-67⁺-TA cells (**g, k**) in the jejunum were also determined. Results are derived from 10 or 12 mice/group (**a–d, h**) or the mean \pm S.D. of 10 tissue sections/mouse (**e–g, i–k**). Kaplan-Meier survival curves were constructed and analyzed by a log rank test (**a, b, d, h**). Bars, 50 μ m. *, $p < 0.05$; **, $p < 0.01$; ****, $p < 0.0001$

Author Manuscript

Author Manuscript

Author Manuscript

Author Manuscript